View metadata, citation and similar papers at core.ac.uk

brought to you by CORE

provided by Texas A&M Repository

JVI Journals.ASM.org

Identification of the Target Cells and Sequence of Infection during Experimental Infection of Ovine Fetuses with Cache Valley Virus

Aline Rodrigues Hoffmann,[a] Christabel Jane Welsh,[a,b] Patricia Wilcox Varner,[a] Andres de la Concha-Bermejillo,[a,c] Judith Marchand Ball,[a] Andy Ambrus,[a] and John Francis Edwards[a]

Department of Veterinary Pathobiology[a] and Department of Veterinary Integrative Biosciences, Texas A&M University, College Station, Texas, USA,[b] and Texas Veterinary Medical Diagnostic Laboratory, College Station, Texas, USA[c]

Cache Valley virus-induced malformations have been previously reproduced in ovine fetuses; however, no studies have established the course of infection of cells and tissues with Cache Valley virus. To address these questions, ovine fetuses at 35 days of gestation were inoculated *in utero* with Cache Valley virus and euthanized at 7, 10, 14, 21, and 28 days postinfection. On postmortem examination, arthrogryposis and oligohydramnios were observed in some infected fetuses. Morphological studies showed necrosis in the central nervous system and skeletal muscle of infected fetuses evaluated after 7 to 14 days postinfection, and hydrocephalus, micromyelia, and muscular loss were observed in infected fetuses after 21 to 28 days postinfection. Using immunohistochemistry and *in situ* hybridization, intense Cache Valley virus antigen and RNA staining was detected in the brain, spinal cord, skeletal muscle, and, to a lesser degree, in fetal membranes and other tissues of infected fetuses. Viral antigen and RNA staining decreased in targeted and infected tissues with the progression of the infection.

Cache Valley virus (CVV) is a mosquito-borne Bunyavirus in the *Orthobunyavirus* genus of the Bunyamwera group that is endemic in the United States and that causes abortion, fetal death, and malformations in small ruminants (11–13, 16, 19, 20). The *Orthobunyavirus* genus also includes Akabane virus and Aino virus, which are associated with abortions and fetal malformations in cattle and sheep (4, 48, 49). CVV also infects a variety of animal species, including horses (6, 32, 39), deer (5, 41), goats, pigs, and caribou (15). In humans, CVV can cause encephalitis and meningitis (7, 50). Outbreaks of CVV with dramatic fetal lamb losses have been reported (11–13, 16, 20).

Ovine fetuses infected with CVV or Akabane virus have a narrow window of susceptibility to infection, and virus can be recovered from tissues before development of immunocompetency, which occurs around 70 to 75 days of gestation (dg) (38, 44), and regardless of the time of infection. However, fetal death, stillbirths, and congenital malformations, such as hydrocephalus, hydranencephaly, microencephaly, porencephaly, torticollis, scoliosis, and arthrogryposis, were reproduced experimentally only when CVV was inoculated between days 29 and 47 of gestation (11, 12, 15, 16, 20). Similarly, fetal malformations have been reproduced experimentally when Akabane virus was inoculated at 30 to 50 dg (29, 42), and if the fetus survived the infection, lambs were born with central nervous system (CNS) and skeletal muscle (SKM) malformations (8, 34, 42).

Although previous studies have reproduced CVV-induced malformations in ovine fetuses (12, 16), those studies did not characterize the early histologic lesions and did not identify the cells targeted by the virus during early infection. The objective of this study was to determine the early lesions and infection sequence of cells infected by CVV in the ovine fetus in order to correlate the early lesions with the CNS and SKM malformations seen in spontaneously affected lambs.

MATERIALS AND METHODS

Experimental animals and preparation of viral inoculum. All procedures in this study were conducted using protocols approved by the University Biosafety and Animal Use Committees. The estrous cycles of fifteen CVV-seronegative Rambouillet ewes were synchronized, and the ewes were bred naturally to a CVV-seronegative ram, as described previously (12). Pregnancies were confirmed by ultrasound examination at postbreeding day (pbd) 33. On pbd 35, the pregnant ewes were transferred to an insect-proof, biosafety level 2 (BSL2), confinement building, and the amniotic cavity of all fetuses was inoculated with a 1-ml inoculum containing 10^5 50% tissue culture-infective doses ($TCID_{50}$s) of CVV (infected group) or with 1 ml of minimum essential medium (MEM) (mock-infected control group), as previously described (11, 12, 19). The virus isolate used in this study was collected from the allantoic membrane of an ewe experimentally inoculated with a low passage of a CVV isolate (CK-102) obtained in 1987 from a sentinel sheep in San Angelo, TX (12). The CVV inoculum was prepared using CVV-infected Vero cells via standard virologic techniques (36). The virus-infected and mock-infected ewes were housed in separate, insect-proof, confinement buildings. The experimental ewes were monitored for clinical signs of disease three times daily, and heparinized blood samples were collected by venipuncture prior to inoculation, and then every 12 h after infection for the first 4 days, and finally on the last day before euthanasia. Whole-blood and serum samples collected for virus isolation and determination of serum neutralizing antibodies, respectively, were stored at −80°C immediately after collection.

Necropsy, sample collection, tissue preparation, and light microscopic tissue examination. At 7, 10, 14, 21, and 28 days postinfection (dpi), three ewes (one mock infected and two CVV infected) were humanely euthanized. The abdominal cavity was opened, and the uterus and fetal membranes were exposed. Macroscopic lesions were noted, and fetal tissues, amniotic and allantoic fluids, and placenta were harvested for testing. One set of fresh, unfixed samples of brain (BRA), spinal cord (SPC), SKM, cotyledons, fetal membranes, and amniotic and allantoic fluids were collected from each fetus at necropsy and frozen at −80°C for

Received 20 November 2011 Accepted 22 February 2012

Published ahead of print 29 February 2012

Address correspondence to Aline Rodrigues Hoffmann, arodrigues@cvm.tamu.edu, or John Francis Edwards, jedwards@cvm.tamu.edu.

Copyright © 2012, American Society for Microbiology. All Rights Reserved.

doi:10.1128/JVI.06858-11

Downloaded from http://jvi.asm.org/ on September 12, 2018 by guest

viral isolation. A second set of fresh, unfixed tissues were placed in an RNA stabilization solution (RNAlater, Ambion Life Technologies, Carlsbad, CA) for PCR assays. Parallel samples of fetal tissues and fetal membranes from up to 21-dpi fetuses were fixed overnight in 4% paraformaldehyde or in Davidson's AFA (acetic acid, formalin, and alcohol) fixative in order to conduct a comparative study of each fixative's performance using immunohistochemistry (IHC) and *in situ* hybridization (ISH) techniques. All samples collected from 28-dpi fetuses were fixed in 4% paraformaldehyde. After fixation, tissues were paraffin embedded and sectioned at 5 μm for routine light microscopy using hematoxylin and eosin staining, as well as for IHC and for ISH. Histologic sections stained with hematoxylin and eosin staining were evaluated for lesions by light microscopy. The distribution of the microscopic lesions observed in the BRA was based on previously described ovine fetal BRA anatomy (3).

Development of polyclonal antibody and immunohistochemical analysis for CVV. Purified virus prepared from CVV-infected Vero cell monolayers (46) was submitted to the Proteintech Group, Inc. (Chicago, IL), for development of a purified, rabbit polyclonal antibody against CVV. Briefly, after the CVV-infected Vero cell monolayers developed cytopathic effect, cell lysates were prepared by exposing the infected cells to three freeze-thaw cycles followed by sonication at 42 W for 5 min to enhance release of viral particles. The sonicated monolayers were clarified by centrifugation at 1,500 $\times$ *g* for 15 min. The suspended CVV virions within the resulting supernatant were layered on top of a 20% sucrose cushion and pelleted at 64,000 $\times$ *g* for 1 h (Beckman SW27). The formed pellet was resuspended in Tris-HCl and NaCl buffer and added to a continuous 20% to 60% sucrose gradient at 94,000 $\times$ *g* for 3 h. All formed fractions were collected and layered on top of a 10% sucrose cushion and pelleted at 80,000 $\times$ *g*. All purification steps were conducted at 4°C. Viral protein concentration was determined by the bicinchoninic acid (BCA) protein assay, and the proteins were fractionated on a polyacrylamide gel in the presence of 0.1% sodium dodecyl sulfate (SDS), following the manufacturer's recommendations (Thermo Scientific, Rockford, IL). To establish the sensitivity of the CVV polyclonal antibody and the approximate working dilution range, the polyclonal CVV antibody was used at a concentration of 100 μg/ml on a Western blot assay using CVV-infected cell lysates following the manufacturer's recommendations (R&D Systems, Minneapolis, MN). Subsequently, the purified antibody was used for immunohistochemical evaluation of CVV antigen on deparaffinized sections mounted on positively charged, silanized slides using an automated staining system for immunohistochemistry (DakoCytomation Autostainer, Dako, Carpinteria, CA). Briefly, endogenous enzyme was blocked with hydrogen peroxide. Samples were pretreated with unconjugated avidin and biotin. Nonspecific epitopes were blocked with Background Sniper (Biocare Medical, Concord, CA). Slides were incubated for 30 min with the CVV polyclonal antibody (1:300), followed by incubation for 20 min with the anti-rabbit secondary antibody labeled with horseradish peroxidase (MACH 2; Biocare Medical). Sections were stained with 3,3-diaminobenzidine tetrachloride (DAB; Dako) and counterstained with hematoxylin.

Tissues were blindly evaluated by one person to determine the percentage of infected cells in each examined organ and graded as follows: +, less than 3% of cells positive; ++, between 3 and 15% of cells positive; and +++, more than 15% of cells positive. To evaluate cross-reaction between the anti-CVV antibody and other bunyaviruses, IHC testing also was done on deparaffinized BRA sections of properly stored, formalin-fixed tissue blocks known to contain La Crosse, Main Drain, or San Angelo virus from a previous study (19).

***In situ* hybridization for CVV.** A CVV-specific, digoxigenin (DIG)-labeled, single-stranded DNA probe complementary to the negative strand of CVV was generated as previously described (30, 35, 45). Briefly, RNA was extracted and purified from CVV-infected cell culture fluid using an RNeasy minikit (Qiagen, Valencia, CA). A unique, 530-bp segment from a conserved region of the medium segment of CVV (GenBank accession no. AF082576) was amplified by reverse transcriptase PCR using CVV-specific primers (forward [F], AGC CTA GAT TGT ATA GAC TGT GGA CCA; reverse [R], TTG GAT CAA TTG ATA AAA TAA GGA TTC). To generate a primarily single-stranded, labeled product, a second PCR was conducted on the resulting amplicon, using only the reverse primer in combination with a DIG DNA labeling mix (Roche Diagnostics, Manheim, Germany) according to the manufacturer's instructions.

The ISH assay was conducted on deparaffinized tissue sections mounted on positive-charged, silanized slides (ProbeOn Plus; Fisher Scientific, Pittsburg, PA) as previously described (9). Slides were initially inserted in a slide holder before being exposed to a series of solutions utilizing the capillary gap refill technology of the manual MicroProbe system (Fisher Scientific) with minor modifications to the described protocol. Briefly, following serial hydration steps, the sections were digested with proteinase K (100 μg/ml in phosphate-buffered saline) for 8 min at 37°C, followed by postfixation in 0.4% paraformaldehyde for 10 min at 4°C. The hybridization step was performed using 50 ng of the CVV-specific, DIG-labeled probe in the hybridization cocktail solution (Fisher Scientific, Pittsburg, PA) with an initial 10-min incubation at 100°C followed by a 2-h incubation at 42°C. Unbound probe was removed by decreasing salt washes (2$\times$ to 0.2$\times$ standard saline citrate buffer). To detect bound, DIG-labeled probe, slides were incubated for 1 h at 37°C in an alkaline phosphatase-labeled, anti-DIG antibody solution (Roche Diagnostics) followed by a 30-min incubation in a development solution containing the chromogen substrate nitroblue tetrazolium–5-bromo-4-chloro-3′-indolylphosphate (NBT/BCIP). Finally, slides were dehydrated and counterstained with Bismarck Brown prior to microscopic examination. Evaluation of the distribution of the viral RNA in infected organs was performed as described above for the IHC. In order to evaluate the specificity of the CVV DIG-labeled probe, ISH was also performed on deparaffinized tissue sections from animals infected with the non-CVV bunyaviruses described above.

Virus isolation. Viral isolation from blood and fetal tissues was performed as described previously (12). Inocula included 1:10 MEM suspensions of either fresh fetal tissues, membranes, cotyledons, ewe blood, or amniotic or allantoic fluids. The inocula were layered onto drained monolayers of Vero cells, incubated for 1 h at 37°C, and subsequently flooded with MEM containing 10% fetal bovine serum and incubated at 37°C in 5% CO_2 for 5 days with daily evaluation for cytopathic effect.

Serum neutralization. Serum from experimental ewes was tested for CVV neutralizing antibodies in triplicate using a microtiter, serum neutralization test in 96-well plates as described previously (12). First, the serum samples were inactivated at 56°C for 30 min and then diluted 1:4, 1:8, 1:16, 1:32, 1:64, 1:128, and 1:256 with MEM. Prior to inoculation, the diluted sera were incubated at 37°C for 60 min with an equal volume of 100 $TCID_{50}$s/ml of CVV. After incubation, Vero cell suspensions diluted in MEM were added to virus-antibody mixtures, and the plates were incubated at 37°C in 5% CO_2 for 5 days. Monolayers were evaluated daily for cytopathic effect, and titers were calculated according to the Spearman Karber method (31, 53). Titers above 1:4 were considered positive.

RESULTS

Macroscopic findings. Three fetuses were collected from CVV-infected ewes at 7 and 10 dpi, and four fetuses were collected at 14, 21, and 28 dpi (Table 1). Of the harvested fetuses at 7 dpi, one fetus was grossly normal (viable) and two nonviable fetuses were diffusely dark red with pale red amniotic fluid. Two grossly normal fetuses (viable) and one dark red, nonviable fetus were recovered at 10 dpi (nonviable). At 14 dpi, one fetus was in early stages of mummification, characterized by diffuse fetal dehydration with dark brown, shrunken dried skin and resorption of membrane fluids (not included in Table 1), and three fetuses were viable, but one had the amnion closely apposed (oligohydramnios) to the fetal body. All four fetuses at 21 dpi had normal fluid and body color and were considered viable. One of these four fetuses had

Downloaded from http://jvi.asm.org/ on September 12, 2018 by guest

TABLE 1 Gross findings observed in fetuses infected with CVV[a]

Ovine fetus no.	dpi/pbd	Gross finding(s)
1	7/42	NF
2	7/42	Dark red fetus and fluids (dying)
3	7/42	Dark red fetus and fluids (dying)
4	10/45	NF
5	10/45	NF
6	10/45	Dark red fetus and fluids (dead)
7	14/49	NF
8	14/49	Oligohydramnios and kyphosis
9	14/49	NF
10	21/56	NF
11	21/56	Mild concave spinal flexion
12	21/56	Oligohydramnios, torticollis, arthrogryposis, and kyphosis
13	21/56	NF
14	28/63	Oligohydramnios, arthrogryposis, and torticollis
15	28/63	NF
16	28/63	NF

[a] dpi, days postinfection; pbd, postbreeding day; NF, no gross findings.

marked oligohydramnios, torticollis, arthrogryposis, and scoliosis (Fig. 1B), and another fetus had mild kyphosis. Three viable fetuses and one mummified fetus (not included in Table 1) were recovered at 28 dpi. One of these fetuses had moderate oligohydramnios with torticollis and hypercontracted flexed front limbs (arthrogryposis). The control fetuses were grossly normal (not included in Table 1).

Microscopic findings. Most microscopic lesions in infected fetuses were limited to the CNS and SKM system. Multifocal areas of necrosis characterized by accumulation of necrotic debris and not associated with inflammation were observed in the BRA, SPC, and SKM at 7 dpi. Areas of severe necrosis were primarily detected in the matrix zone and mantle layers of the cerebral cortex. In addition, multifocal, scattered areas of necrosis were detected in the brainstem and gray matter of the SPC, especially in the dorsal horns. No vascular lesions or sites of thrombosis were identified. The appendicular and dorsal SKM adjacent to the vertebral column were mainly affected by multifocal discrete necrotic areas.

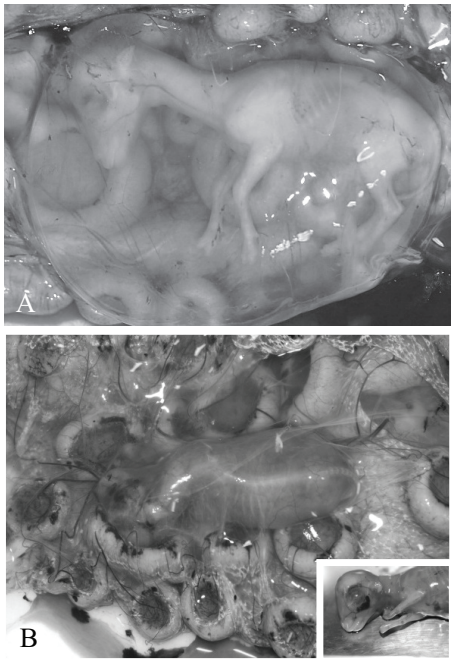

FIG 1 Gross findings in control and infected ovine fetuses. (A) Control fetus at 56 pbd. The fetus floats freely within the amniotic sac. (B) Ovine fetus infected with CVV, 21 dpi (56 pbd). Severe oligohydramnios results in the fetal amnion becoming in close contact with the body of the fetus. The fetus has scoliosis of the cervical and thoracic vertebrae. (Inset) Severe arthrogryposis results in hypercontraction of the limbs.

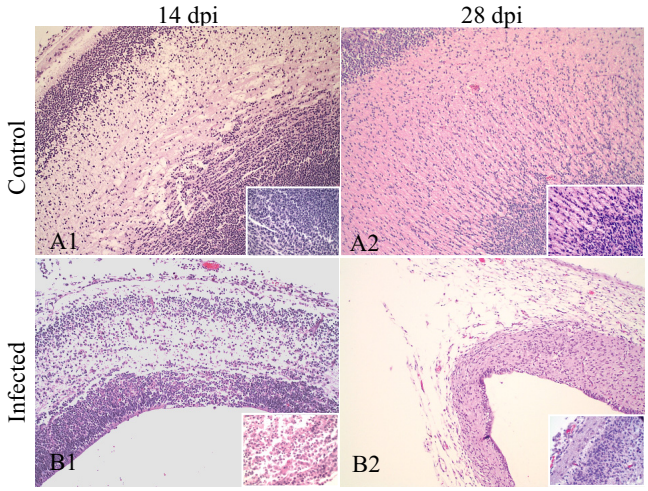

FIG 2 Histology of cerebral cortex of control (A) and CVV-infected (B) fetuses. Necrosis and cell debris are seen at 14 dpi (B1). The cerebral cortex was markedly thinner due to cellular loss at 28 dpi (B2). Hematoxylin and eosin; magnification, 100×; inset magnification, 400×.

At 10 dpi, areas of necrosis were observed affecting the matrix and intermediate zones of the cerebral cortex and brainstem. Moderate necrosis was seen in the dorsal horns of the SPC. Discrete areas of necrosis similar to those observed at 7 dpi were seen in the SKM. In addition, SKM had scattered foci of infiltrating granulocytes between the SKM fibers along with mild, multifocal hemorrhage. Perivascular accumulations of cellular debris were also observed in the fetal membranes of the nonviable fetuses.

At 14 dpi, severe, multifocal areas of necrosis affected all layers of the cerebral cortex and the brainstem, resulting in hydrocephalus *ex vacuo* (Fig. 2B1). The necrosis noted in the SPC was more extensive and severe than that observed at 7 and 10 dpi (Fig. 3B1). An infiltrate of mononuclear cells was observed in the meninges of the BRA and SPC. No significant necrosis was observed in the SKM; however, small aggregates of mononuclear cells and granulocytes were in the SKM (Fig. 4B1), focally in the SKM of the tongue and in the smooth muscle of the intestine. Marked perivascular accumulation of necrotic cellular debris was observed in the amniotic membrane of the mummified fetus.

At 21 dpi, severe necrosis, loss of neuropil, meningeal inflammatory cell infiltrates (meningitis), and hydrocephalus *ex vaccuo* were observed in the BRA. The SPC of three experimentally infected fetuses had marked parenchymal loss and micromyelia. BRA and SPC had multifocal moderate areas of mineralization. Focal mononuclear cell myositis was also observed, along with reduction in the thoracic and lumbar dorsal muscle mass in two fetuses. Findings at 28 dpi were similar to those observed in the

Downloaded from http://jvi.asm.org/ on September 12, 2018 by guest

TABLE 2 Detection of CVV in tissues of infected fetuses at different days postinfection[a]

dpi	Fetus no.	Brain			Spinal cord			Skeletal muscle			Ganglion		Heart		Kidney		Eye		Allantois		Amnion		Allantoic fluid (VI)	Amniotic fluid (VI)
		IHC	ISH	VI	IHC	ISH	VI	IHC	ISH	VI	IHC	ISH	IHC	ISH	IHC	ISH	IHC	ISH	IHC	VI	IHC	VI		
7	1	+++	+++	+[b]	+++	+++		+++	+++	+[b]	+++	+++	+	–	++	+			++	+[b]	+++	+[b]	+	+[b]
	2	+++	+++		+++	+++		+++	+++		+++	+++	+	+	+	+	+	–	++	+[b]	++	+[b]	+[b]	+[b]
	3	+++	+++		+++	+++		+++	+++	+	++	++	–	–	++	++	–	–	+	+	+++	+	+[b]	+
10	4	+++	+++	+[b]	+++	+++	+[b]	+++	+++	+[b]	++	++	++	+	–	+	++	+	–	+	++	+	+[b]	+[b]
	5	+++	+++	+[b]	+++	+++	+[b]	+++	++	+[b]	+	+	++		+	–	++	+		–		+[b]	+[b]	+[b]
	6			+						+										–		+	+	+
14	7	++	+++	+	+++	+++	+[b]	++	+	+[b]	+	–	+	–	+	+	+	+	–	+[b]	+	+[b]	+	+[b]
	8	+++	+++	+[b]	+++	+++	+[b]	+++	+	+[b]	++	+	++	+	++	++	+	+	+	–	+	+[b]	+	+
	9	++	+++	+[b]	+++	+++	+[b]	+++	++	–	+	+	+	–	+	+	++	+	+	+[b]	++	+[b]	+[b]	+[b]
21	10	++	+++	+	++	++	+	+	–	–	+	–	–	–	+	+	+	+	+	–	+	+	+	+
	11	++	++	+[b]	++	+	+[b]	+	–	+	+	–	+	–	+	+	+	+	+	+	+	+		+
	12	+++	+++		+++	+	+[b]	++	++	+[b]	++	+	+	–	++	+	+	+	–	+	+	+	+	+[b]
	13	++	++	+[b]	++	+	+[b]	++	+	+[b]	+	+	+	–	+	+	+	–		+	++		+	–
28	14	++	++	+[b]	+	+	+[b]	+	–	+	–	–	+	–	+	–	+	+	–	–	+	+	+	–
	15	++	++	+[b]	+	+	–	+	+	–	+	–	+	–	+	–	+	+	–	+	–	+	+	+
	16	+	+	+[b]	–	+	–	–	–	+	–	–	–	–		–			–	+	++	+	+[b]	+

[a] dpi, days postinfection; IHC, immunohistochemistry; ISH, *in situ* hybridization; VI, viral isolation.
[b] Virus was isolated at the 1st passage. Blank spaces indicate samples that were not examined.

FIG 3 Histology of thoracic spinal cord of control (A) and CVV-infected (B) fetuses. Necrosis and cell debris are seen at 14 dpi (B1). Progressive cellular and parenchyma loss results in micromyelia, as noted at 28 dpi (B2). Hematoxylin and eosin; magnification, 100×.

SPC, BRA, and SKM of fetuses at 21 dpi. However, less necrotic debris was detected in the BRA and SPC, but the hydrocephalus and micromyelia were more apparent (Fig. 2B2 and 3B2). Moderate reduction in the dorsal SKM mass was observed in one of the fetuses at 28 dpi (Fig. 4B2). Additionally, one fetus had minimal, focal necrosis in tubular epithelial cells of the renal cortex. Hypercontraction bands and mild mononuclear perivascular and interstitial infiltrates were observed in the SKM of both control and infected fetuses at 21 and 28 dpi; however, most infected fetuses had slightly greater numbers of mononuclear cells.

Distribution of IHC viral antigen in fetuses infected with CVV. The IHC CVV antigen in infected fetuses is shown in Table 2. The results were identical for tissues fixed in both fixatives. The tissues with abundant viral antigen included the BRA, SPC, and

FIG 4 Histology of skeletal muscle of control fetuses (A) and infected fetuses with arthrogryposis (B). Scattered areas of inflammation composed of granulocytes and mild hemorrhage are within myofibers of a 14-dpi fetus (B1). At 28 dpi (B2), loss of myofibers is evident in the muscles around vertebrae. Hematoxylin and eosin; magnification, 400×.

Downloaded from http://jvi.asm.org/ on September 12, 2018 by guest

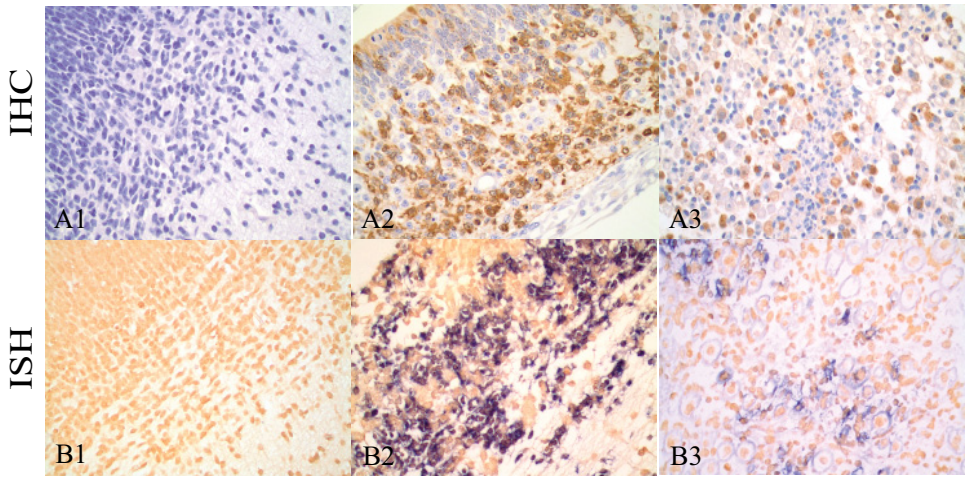

FIG 5 Immunohistochemistry and *in situ* hybridization in brain and skeletal muscle. A rabbit polyclonal antibody against CVV and stained with DAB chromogen (brown) was used to detect CVV antigen in the brain of a control fetus (A1) and an infected fetus (A2) and in the skeletal muscle of an infected fetus at 14 dpi (A3). *In situ* hybridization using a digoxigenin-labeled DNA probe complementary to a conserved region of the CVV M gene glycoprotein 1 and labeled with NBT/BCIP (blue) was performed in brain from control (B1) and infected (B2) fetuses and skeletal muscle from an infected fetus at 14 dpi (B3). No viral antigen and RNA are detected in the brain of the control fetus (A1 and B1). Numerous cells in the brain (A2 and B2) and skeletal muscle (A3 and B3) are positive for CVV antigen (A2 and A3) and for the CVV M glycoprotein 1 (B2 and B3). Magnification, 400×.

SKM, with the antigen primarily associated with necrotic foci. Within the BRA, the distribution of intense viral antigen was diffuse within the cerebral cortex at 7 and 10 dpi. At 14 dpi, viral antigen was mainly distributed within the matrix zone (Fig. 5A2), and at 21 dpi, viral antigen was mainly distributed within the mantle and primordial layers. Only scattered foci had positive cells throughout the cerebral cortex at 21 dpi. The SPC had intense and diffuse viral antigen distribution throughout the cervical, thoracic, and lumbar levels of the SPC. At 7 and 10 dpi, viral antigen was distributed in both the dorsal and ventral aspects of the SPC and primarily within the dorsal aspect after 14 dpi. CVV antigen was identified often in myofibers in the developing SKM around the vertebrae and ribs (Fig. 5A3), with slightly fewer myofibers being positive within the SKM of the front and hind limbs, especially after 21 and 28 dpi. Virus-positive cells were cleared from SKM earlier than from the CNS. Positive cells were observed in the ganglion cells of the dorsal root ganglia, neuron layer of the retina, in cardiomyocytes, and in the renal tubular and glomerular epithelium. Occasionally, CVV antigen-positive cells were seen in the media of the aorta, in lymph nodes, and in the spleen. Scattered mesenchymal cells in the fetal membranes were positive, with the amniotic membranes being more intensely affected than the allantoic membranes. CVV antigen was infrequently detected in amniotic epithelial cells and was detected in the trophoblastic cells of the cotyledons in only one fetus at 7 dpi. A progressive decrease in viral antigen was observed in most affected tissues as the infection progressed, with rare positive cells noted in tissues at 28 dpi. CVV antigen was not observed in tissues collected from control animals and in tissues of animals infected with other orthobunyaviruses.

Distribution of ISH CVV viral RNA in fetuses infected with CVV. For the most part, the tissue distribution of CVV-nucleic acid detected by ISH was identical to the tissue distribution of CVV antigen detected by IHC (Table 2). The type of fixative used appeared to have no effect on the intensity or quality of the viral RNA staining. Similar to the results observed with the IHC, the tissues with most abundant viral RNA were BRA (Fig. 5B2), SPC, and SKM (Fig. 5B3). The distribution and quantity of viral RNA in other tissues were similar to those observed with IHC, although the level of viral RNA appeared reduced in comparison to that observed with IHC. Tissues collected from fetuses during the earlier postinfection had more intense viral RNA staining than those collected later postinfection. CVV nucleic acid was not detected by ISH in fetal membranes. ISH viral RNA was not observed in tissues collected from control animals or from animals infected with other bunyaviruses.

Viral isolation. The results of CVV isolation are summarized in Table 2. Virus was isolated from most examined fetal tissues, except for the cotyledons, where virus was isolated only from one 7-day-infected fetus on 3rd passage. CVV was isolated on 1st passage mainly from BRA and SPC, as well as from amniotic fluids and membranes. No virus was isolated from blood collected from infected ewes. No virus was isolated in any of the tissues collected from control animals.

Serum neutralization. All infected ewes developed antibodies to CVV, except for one ewe euthanized at 7 dpi. On the day of euthanasia, the serum neutralizing antibody titers for infected ewes were 1:16 at 7 dpi, 1:8 and 1:32 at 10 dpi, 1:16 and 1:32 at 14 dpi, 1:32 and 1:64 at 21 dpi, and 1:64 and 1:128 at 28 dpi. None of the control animals developed antibodies to CVV.

DISCUSSION

This study focused on CVV-induced macroscopic and microscopic lesions and on the distribution of CVV in affected tissues from ovine fetuses experimentally infected at pbd 35 and sequentially collected at 7, 10, 14, 21, and 28 dpi. The macroscopic and microscopic lesions in CVV experimentally infected ovine fetuses correlated to the lesions observed in natural CVV infections (11, 13, 16). Although CVV experimental infection studies using the intrauterine route of inoculation have resulted in the same macroscopic and microscopic fetal lesions as those in naturally CVV-infected ovine fetuses (12, 16, 19), the sequential distribution and identification of the infected cell populations have not been re-

Downloaded from http://jvi.asm.org/ on September 12, 2018 by guest

ported. Fetal infection is generally unsuccessful when pregnant ewes are experimentally infected with CVV by the intravenous route, even when ewes are inoculated with high doses of low-passage virus (18). Although experimental intravenous infection of pregnant ewes with Akabane virus can be more successful at fetal infection than CVV, the fetal infection rate has also been low in some studies (34, 43). The reason for the low rate of fetal infection when pregnant ewes are experimentally infected by the intravenous route with arboviruses is uncertain. It has been speculated that effector molecules in the saliva of the infected vector during natural infection may be a key feature of arbovirus pathogenesis (18). Because of the low rate of fetal infection when pregnant ewes are experimentally infected intravenously and in order to reduce the number of animals used in this study, the intrauterine route was used. The use of this route of inoculation did not influence the development of fetal malformations, as lesions correlated well with those seen in natural infections. However, the use of this route of inoculation perhaps influenced the viral distribution in placental tissues.

The data found in this study support the hypothesis that the fetal CNS and SKM are targeted during CVV infection. CVV-infected cells were detected both by IHC and by ISH in association with areas of necrosis in the BRA, SKM, and SPC of experimentally infected ovine fetuses. CVV antigen, RNA, and infectious virus corresponded with the sites of development of hydrocephalus, porencephaly, micromyelia, and body malformations, as well as with the lesion descriptions reported in affected lambs from natural CVV outbreaks. Viral antigen and RNA were also observed in other cells of the peripheral nervous system, including the ocular retinal cells and in ganglion cells in the dorsal root ganglia, but these lesions have not been described in natural cases of CVV-malformed lambs. In natural and experimental cases of CVV (20) and Akabane virus (8, 33, 34, 42), lesions in the SPC are found in both the dorsal and ventral horns, with slightly more severe lesions involving the ventral motor neurons. In this study, most fetuses at 7 to 14 dpi had more severe microscopic lesions and intense staining for CVV antigen and RNA in the dorsal horns, even though in the fetuses at 21 and 28 dpi, the loss of SPC parenchyma affected both the dorsal and ventral horns and caused severe micromyelia. Based on the findings of this study, it is likely that the CVV-induced SKM lesions result both from direct infection of myofibers as well as from denervation atrophy. In addition to the CVV tropism for the SKM, viral antigen and RNA, but without necrosis, were seen in the cardiac muscle and smooth muscle of the gastrointestinal tract of some fetuses. Hypercontraction bands and scattered perivascular and interstitial mononuclear cellular infiltrates observed in SKM of fetuses at 21 and 28 dpi are likely developmental changes in ovine fetuses, since these changes were observed in both control and infected fetuses.

Fetal membranes and placental fluids have been shown to contain virus in early CVV infection (11, 15, 16, 19). In our study, CVV was isolated from and persisted in the fetal membranes and fluids throughout the course of infection. Using IHC, viral antigens were seen in mesenchymal cells of the amniotic and allantoic membranes and only occasionally in epithelial cells of the amniotic membrane. As time postinfection increased, fewer mesenchymal cells were seen to be infected, but virus was still isolated from fetal membranes and fluids until 28 dpi. Although functional testing of the membranes was not done, it may be speculated that viral infection disrupts the intramembranous movement of fluid in the amnion and contributes to the oligohydramnios. In ovine fetuses, the intramembranous pathway is considered a major route of absorption of water from the amniotic cavity (21, 23–25). CVV RNA was not detected by ISH in fetal membranes. This lack of viral RNA may correlate with viral RNA degradation associated with prolonged storage of these delicate specimens in the fixative solution prior to transfer to ethanol and subsequent tissue processing. Use of shorter fixation times for this assay would be recommended in future studies. Conceivably, phagocytic mesenchymal cells in the placenta could be phagocytizing viral particles, resulting in degradation of viral RNA, but preservation of protein, and consequent lack of identification of viral RNA in placental tissues.

In previous experimental infections with CVV, virus was routinely isolated from cotyledons (12, 13), but in the present study, infectious virus was detected in the fetal cotyledon of only one experimentally infected fetus, and only rare trophoblastic cells had cytoplasmic viral antigen in another experimentally infected fetus. It is possible that the greater success rate of virus isolation from the fetal cotyledons in previous studies was the result of cross-contamination due to the intimate contact with the fetal membranes and fetal fluids containing high titers of virus. The limited involvement of trophoblasts in the cotyledons in this experimental infection presumably reflects the artificial intrauterine route of fetal infection. Successful intravenous infection of pregnant ewes with Akabane virus has been shown to cause more severe necrotic changes associated with detection of the viral antigen in the trophoblastic cells and placentomes (43).

One cause of congenital limb and axial skeletal malformations is decreased fetal movement (fetal akinesia) (1, 26, 27, 40, 47, 51, 52) associated with oligohydramnios. Spinal flexion with resulting increased pulmonary/abdominal compression and diaphragmatic displacement have been described in ovine fetuses with experimentally induced oligohydramnios produced by drainage of amniotic and allantoic fluids in late gestation (28). Based on experimental studies with ovine fetal fluid drainage and the demonstration of CVV-induced oligohydramnios (16, 17), fetal akinesia could play a role in the pathogenesis of the SKM deformities observed in CVV infection. Many processes may affect amniotic fluid volume. For example, experiments performed in ovine fetuses have also demonstrated that severe placental insufficiency results in fetal hypoxia and hypercapnia, which alters the amniotic fluid composition and can be associated with the development of oligohydramnios (22). The association of severe viral infection with development of oligohydramnios has only been reported with ovine CVV infection. In the present study, three infected fetuses displayed severe oligohydramnios with axial and limb deformities relatively early in fetal life. Obviously, the CNS and SKM lesions induced by CVV must contribute to these lesions. Abnormalities affecting the central and peripheral nervous systems are actually considered to be the most common cause of decreased fetal movement in affected fetuses with subsequent development of arthrogryposis (26). In this study, one infected animal at 21 dpi had kyphosis, without oligohydramnios. The combined effect of the CNS and SKM lesions and oligohydramnios early in fetal development could explain the severe axial and limb malformations often seen in lambs born after CVV intrauterine infection. Even though oligohydramnios has not been described in experimental Akabane virus infections, lung hypoplasia, a component of the "oligohydramnios tetrad" associated with oligohydramnios in human fetuses (47, 54, 55), has been seen in some ovine fetuses experimen-

Downloaded from http://jvi.asm.org/ on September 12, 2018 by guest

tally infected with Akabane virus (42). It would be important to determine if oligohydramnios occurs with other bunyaviral infections.

Oligohydramnios resulting from fetal renal failure also needs to be considered in the pathogenesis of oligohydramnios. In this study, CVV-infected cells were found scattered in fetal renal tubules and glomerulae at different dpi, and minimal tubular epithelial cell necrosis was only observed in one fetus at 28 dpi. The origin and control of amniotic fluid during early gestation of ovine fetuses have not been completely elucidated. However, because the amniotic fluid during early gestation is believed to be primarily an ultrafiltrate of fetal blood plasma, renal disease could possibly affect amniotic fluid volume (10, 37). The ovine fetal mesonephros is able to produce urine that is excreted into the allantoic cavity as early as 30 dg (14, 57, 58). The vast majority of the urine produced in early gestation is primarily transferred to the allantoic cavity from the urinary bladder via the urachus (2, 56, 58). If the possibility that the fetal urine production also contributes to the formation of the amniotic fluid in early gestation is considered, even mild infection of the fetal kidney could possibly affect fetal urine production and consequentially contribute to oligohydramnios.

The IHC and ISH protocols developed in this study to identify CVV in tissues of experimentally infected ovine fetuses could be further used for diagnostic purposes to confirm or rule out natural cases of CVV on properly collected tissues. Both techniques did not cross-react with three other orthobunyaviruses in brain from experimentally infected fetuses, and, therefore, the primary antibody and probe generated could be used to differentiate between CVV and other bunyaviruses. Certainly in areas where other bunyaviruses are active, it would be advisable to test the specificity of the anti-CVV polyclonal antibody used in this study. In terms of sensitivity, the IHC seemed more sensitive than ISH and detected viral antigens in some infected tissues in which CVV RNA was not detected by ISH. Additionally, IHC frequently detected a higher percentage of cells infected with CVV in different tissues. However, the sensitivity of IHC and ISH to detect CVV in tissues of infected fetuses may be improved by reducing fixation times, particularly in fetal membranes. Conceivably, phagocytic mesenchymal cells in the placenta could be phagocytizing viral particles, resulting in degradation of viral RNA, but preservation of protein, and consequent lack of identification of viral RNA in placental tissues. Both IHC and ISH represent excellent tools for use in further experimental studies, as well as for diagnostic purposes in the detection of CVV in early abortions.

CVV is a viral pathogen with a tropism for the ovine fetal CNS, SKM, and fetal membranes. The study of early infection demonstrated a tropism that correlated well with the CNS and SKM malformations observed in spontaneous CVV disease. With CVV, the development of arthrogryposis probably has a multifactorial pathogenesis involving effects on developing neurons, myocytes, and fetal membranes. Since CVV is the only viral infection that has been shown to cause oligohydramnios, it has potential to serve as an animal model for experimental pathogenesis studies of this condition in both animals and humans. This study further characterizes the CVV viral fetal model of oligohydramnios and development of SKM malformations in fetuses.

ACKNOWLEDGMENTS

This study was supported by USDA Animal Formula Health Research Grant AH-9249.

We thank Rebecca Parr, Yaping Fan, and the staff of the histology laboratory of the Department of Veterinary Pathobiology, Texas A&M University for excellent technical support.

REFERENCES

1. **Albuquerque CA, et al.** 2002. Relation between oligohydramnios and spinal flexion in the human fetus. Early Hum. Dev. **68**:119–126.
2. **Alexander DP, Nixon DA, Widdas WF, Wohlzogen FX.** 1958. Gestational variations in the composition of the foetal fluids and foetal urine in the sheep. J. Physiol. **140**:1–13.
3. **Astrom K.** 1967. On the early development of the isocortex in fetal sheep. Prog. Brain Res. **26**:1–59.
4. **Beaty BJ, Calisher CH.** 1991. *Bunyaviridae*—natural history. Curr. Top. Microbiol. Immunol. **169**:27–78.
5. **Blackmore CG, Grimstad PR.** 1998. Cache Valley and Potosi viruses (*Bunyaviridae*) in white-tailed deer (*Odocoileus virginianus*): experimental infections and antibody prevalence in natural populations. Am. J. Trop. Med. Hyg. **59**:704–709.
6. **Camara A, Contigiani MS, Medeot SI.** 1990. Concomitant activity of 2 bunyaviruses in horses in Argentina. Rev. Argent. Microbiol. **22**:98–101.
7. **Campbell GL, et al.** 2006. Second human case of Cache Valley virus disease. Emerg. Infect. Dis. **12**:854–856.
8. **Charles JA.** 1994. Akabane virus. Vet. Clin. North Am. Food Anim. Pract. **10**:525–546.
9. **Chenggis ML, Unger ER.** 1993. Application of a manual capillary action workstation to colorimetric in situ hybridization. J. Histotechnol. **16**:33–38.
10. **Chiboka O, Thomas KD.** 1985. Changes in the blood and foetal fluid composition at different stages of gestation in ewes. Beitr. Trop. Landwirtsch. Vetmed. **23**:65–71.
11. **Chung SI, et al.** 1990. Evidence that Cache Valley virus induces congenital malformations in sheep. Vet. Microbiol. **21**:297–307.
12. **Chung SI, Livingston CW, Jr, Edwards JF, Gauer BB, Collisson EW.** 1990. Congenital malformations in sheep resulting from in utero inoculation of Cache Valley virus. Am. J. Vet. Res. **51**:1645–1648.
13. **Chung SI, Livingston CW, Jr, Jones CW, Collisson EW.** 1991. Cache Valley virus infection in Texas sheep flocks. J. Am. Vet. Med. Assoc. **199**:337–340.
14. **Davies J.** 1952. Correlated anatomical and histochemical studies on the mesonephros and placenta of the sheep. Am. J. Anat. **91**:263–299.
15. **de la Concha-Bermejillo A.** 2003. Cache Valley Virus is a cause of fetal malformation and pregnancy loss in sheep. Small Ruminant Res. **49**:1–9.
16. **Edwards JF.** 1994. Cache Valley Virus. Vet. Clin. North Am. Food Anim. Pract. **10**:515–524.
17. **Edwards JF, Hendricks K.** 1997. Lack of serologic evidence for an association between Cache Valley Virus infection and anencephaly and other neural tube defects in Texas. Emerg. Infect. Dis. **3**:195–197.
18. **Edwards JF, Higgs S, Beaty BJ.** 1998. Mosquito feeding-induced enhancement of Cache Valley Virus (*Bunyaviridae*) infection in mice. J. Med. Entomol. **35**:261–265.
19. **Edwards JF, Karabatsos N, Collisson EW, de la Concha-Bermejillo A.** 1997. Ovine fetal malformations induced by in utero inoculation with Main Drain, San Angelo, and LaCrosse viruses. Am. J. Trop. Med. Hyg. **56**:171–176.
20. **Edwards JF, Livingston CW, Chung SI, Collisson EC.** 1989. Ovine arthrogryposis and central nervous system malformations associated with in utero Cache Valley virus infection: spontaneous disease. Vet. Pathol. **26**:33–39.
21. **Faichney GJ, Fawcett AA, Boston RC.** 2004. Water exchange between the pregnant ewe, the foetus and its amniotic and allantoic fluids. J. Comp. Physiol. B **174**:503–510.
22. **Gagnon R, Harding R, Brace RA.** 2002. Amniotic fluid and fetal urinary responses to severe placental insufficiency in sheep. Am. J. Obstet. Gynecol. **186**:1076–1084.
23. **Gilbert WM.** 1999. Allantoic fluid compositional changes during acute urine drainage in fetal sheep. J. Soc. Gynecol. Invest. **6**:17–21.
24. **Gilbert WM, Brace RA.** 1989. The missing link in amniotic fluid volume regulation: intramembranous absorption. Obstet. Gynecol. **74**:748–754.
25. **Gilbert WM, Brace RA.** 1990. Novel determination of filtration coefficient of ovine placenta and intramembranous pathway. Am. J. Physiol. **259**:R1281–R1288.
26. **Hall JG.** 1997. Arthrogryposis multiplex congenita: etiology, genetics,

Downloaded from http://jvi.asm.org/ on September 12, 2018 by guest

classification, diagnostic approach, and general aspects. J. Pediatr. Orthop B. **6**:159–166.
27. **Hall JG.** 2009. Pena-Shokeir phenotype (fetal akinesia deformation sequence) revisited. Birth Defects Res. A Clin. Mol. Teratol. **85**:677–694.
28. **Harding R, Hooper SB, Dickson KA.** 1990. A mechanism leading to reduced lung expansion and lung hypoplasia in fetal sheep during oligohydramnios. Am. J. Obstet. Gynecol. **163**:1904–1913.
29. **Hashiguchi Y, Nanba K, Kumagai T.** 1979. Congenital abnormalities in newborn lambs following Akabane virus infection in pregnant ewes. Natl. Inst. Anim. Health Q. (Tokyo) **19**:1–11.
30. **Kanno H, et al.** 2005. Vascular lesion in a patient of chronic active Epstein-Barr virus infection with hypersensitivity to mosquito bites: vasculitis induced by mosquito bite with the infiltration of nonneoplastic Epstein-Barr virus-positive cells and subsequent development of natural killer/T-cell lymphoma with angiodestruction. Hum. Pathol. **36**:212–218.
31. **Karber G.** 1939. Beitrag zur kollektiven behandlung pharmakologischer reihenversuche. Naunyn Schmiedebergs Arch. Exp. Pathol. Pharmakol. **152**:480–483.
32. **Kokernot RH, et al.** 1969. Arbovirus studies in the Ohio-Mississippi Basin, 1964–1967. IV. Cache Valley virus. Am. J. Trop. Med. Hyg. **18**:768–773.
33. **Konno S, Moriwaki M, Nakagawa M.** 1982. Akabane disease in cattle: congenital abnormalities caused by viral infection. Spontaneous disease. Vet. Pathol. **19**:246–266.
34. **Konno S, Nakagawa M.** 1982. Akabane disease in cattle: congenital abnormalities caused by viral infection. Experimental disease. Vet. Pathol. **19**:267–279.
35. **Latimer KS, et al.** 1997. Diagnosis of avian adenovirus infections using DNA in situ hybridization. Avian Dis. **41**:773–782.
36. **Mahy BWJ, Okangro H.** 1996. Virology methods manual. Academic Press, San Diego, CA.
37. **Malan AI, Malan AP.** 1937. The influence of age on (a) amount and (b) nature and composition of the allantoic and amniotic fluids of the merino ewe. Onderstepoort J. Vet. Sci. Anim. Ind. **9**:205–218.
38. **McClure S, et al.** 1988. Maturation of immunological reactivity in the fetal lamb infected with Akabane virus. J. Comp. Pathol. **99**:133–143.
39. **McLean RG, Calisher CH, Parham GL.** 1987. Isolation of Cache Valley virus and detection of antibody for selected arboviruses in Michigan horses in 1980. Am. J. Vet. Res. **48**:1039–1041.
40. **Moessinger AC.** 1983. Fetal akinesia deformation sequence: an animal model. Pediatrics **72**:857–863.
41. **Neitzel DF, Grimstad PR.** 1991. Serological evidence of California group and Cache Valley virus infection in Minnesota white-tailed deer. J. Wildl. Dis. **27**:230–237.
42. **Parsonson IM, Della-Porta AJ, Snowdon WA.** 1981. Akabane virus infection in the pregnant ewe. 2. Pathology of the foetus. Vet. Microbiol. **6**:209–224.
43. **Parsonson IM, McPhee DA, Della-Porta AJ, McClure S, McCullagh P.** 1988. Transmission of Akabane virus from the ewe to the early fetus (32 to 53 days). J. Comp. Pathol. **99**:215–227.
44. **Popp SK, et al.** 2007. Transient transmission of porcine endogenous retrovirus to fetal lambs after pig islet tissue xenotransplantation. Immunol. Cell Biol. **85**:238–248.
45. **Ramis A, Latimer KS, Gibert X, Campagnoli R.** 1998. A concurrent outbreak of psittacine beak and feather disease virus, and avian polyomavirus infection in budgerigars (Melopsittacus undulatus). Avian Pathol. **27**:43–50.
46. **Ranki M, Pettersson RF.** 1975. Uukuniemi virus contains an RNA polymerase. J. Virol. **16**:1420–1425.
47. **Richards DS.** 1991. Complications of prolonged PROM and oligohydramnios. Clin. Obstet. Gynecol. **34**:759–768.
48. **Schmaljohn CS.** 1996. *Bunyaviridae*: the viruses and their replication, p 649–673. *In* Fields BN, Knipe DM, Howley PM (ed), Fundamental virology, 3rd ed. Lippincott-Raven, Philadelphia, PA.
49. **Schmaljohn CS, Nichol ST (ed).** 2007. *Bunyaviridae*, 5th ed, vol 2. Lippincott Williams & Wilkins, Philadelphia, PA.
50. **Sexton DJ, et al.** 1997. Life-threatening Cache Valley virus infection. N. Engl. J. Med. **336**:547–549.
51. **Sherer DM, Spong CY, Minior VK, Salafia CM.** 1996. Decreased amniotic fluid volume at <32 weeks of gestation is associated with decreased fetal movements. Am. J. Perinatol. **13**:479–482.
52. **Sival DA, Visser GHA, Prechtl HFR.** 1990. Does reduction of amniotic fluid affect fetal movements? Early Hum. Dev. **23**:233–246.
53. **Spearman C.** 1908. The method of "right or wrong cases" (constant stimuli) without Gauss's formulae. Br. J. Psychol. **2**:227–242.
54. **Swinyard CA, Bleck EE.** 1985. The etiology of arthrogryposis (multiple congenital contracture). Clin. Orthop. Related Res. **194**:15–29.
55. **Thomas IT, Smith DW.** 1974. Oligohydramnios, cause of the nonrenal features of Potter's syndrome, including pulmonary hypoplasia. J. Pediatr. **84**:811–815.
56. **Wales RG, Murdoch RN.** 1973. Changes in the composition of sheep fetal fluids during early pregnancy. J. Reprod. Fertil. **33**:197–205.
57. **Wintour EM, et al.** 1996. Ontogeny of hormonal and excretory function of the meso- and metanephros in the ovine fetus. Kidney Int. **50**:1624–1633.
58. **Wintour EM, Laurence BM, Lingwood BE.** 1986. Anatomy, physiology and pathology of the amniotic and allantoic compartments in the sheep and cow. Aust. Vet. J. **63**:216–221.

Downloaded from http://jvi.asm.org/ on September 12, 2018 by guest